



**Get Clarity On Generics**

Cost-Effective CT & MRI Contrast Agents

**FRESENIUS  
KABI**

**WATCH VIDEO**

**AJNR**








This information is current as  
of August 4, 2025.

**Peritumoral Hyperintense Signal on  
Postcontrast FLAIR Images Surrounding  
Vestibular Schwannomas Following  
Stereotactic Radiosurgery**

Sandy T. Nguyen, John C. Benson, Girish Bathla, Paul J.  
Farnsworth, Matthew L. Carlson, Michael J. Link and John I.  
Lane

*AJNR Am J Neuroradiol* published online 13 January 2025  
<http://www.ajnr.org/content/early/2025/06/05/ajnr.A8657>

# Peritumoral Hyperintense Signal on Postcontrast FLAIR Images Surrounding Vestibular Schwannomas Following Stereotactic Radiosurgery

 Sandy T. Nguyen,  John C. Benson,  Girish Bathla,  Paul J. Farnsworth,  Matthew L. Carlson,  Michael J. Link, and  John I. Lane

## ABSTRACT

**BACKGROUND AND PURPOSE:** Prior investigations have noted the presence of peritumoral hyperintense signal (a “halo”) around vestibular schwannomas on postcontrast 3D T2 FLAIR images. This study evaluated this phenomenon in a cohort of patients undergoing stereotactic radiosurgery.

**MATERIALS AND METHODS:** A retrospective review was completed of consecutive patients with presumed vestibular schwannomas undergoing stereotactic radiosurgery. Tumor size, location, presence or absence of a peritumoral halo, and halo thickness were recorded. Images were reviewed for presence and size of peritumoral hyperintense signal on postcontrast 3D T2 FLAIR images before and after treatment.

**RESULTS:** Twenty-six patients were included in this study, 14 of whom were women (54.0%). Average age was  $62 \pm 12$  years. Before treatment, a postcontrast 3D T2 FLAIR hyperintense peritumoral halo was seen in 85% of patients, averaging  $0.8 \pm 0.4$  mm in thickness. There was a higher incidence of peritumoral halo in posttreatment patients (96%) than pretreatment patients (85%) ( $P = .017$ ) with a mean follow-up period of 1.2 years (SD 0.35) from November 12, 2019, to September 5, 2023. The average halo thickness was also larger in posttreatment patients (average  $=1.4 \pm 0.4$  mm) compared with pretreatment patients ( $0.8 \pm 0.4$  mm) ( $P < .001$ ). Average tumoral size did not significantly change following treatment ( $P = .10$ ).

**CONCLUSIONS:** Vestibular schwannomas treated with stereotactic radiosurgery are more likely to have a peritumoral halo on postcontrast 3D T2 FLAIR images, with larger halo size as compared with pretreatment studies. Further study with a larger tumor cohort and longer follow-up will be necessary to determine if these findings are predictive of subsequent tumor shrinkage.

**ABBREVIATIONS:** CPA = cerebellopontine angle; IAC = internal auditory canal; SRS = stereotactic radiosurgery; VS = vestibular schwannoma

Vestibular schwannomas (VSs) are benign nerve sheath tumors that account for 6%–8% of all intracranial tumors and represent the most common tumor of the cerebellopontine angle (CPA). VSs classically arise within the internal auditory canal (IAC) and extend into the CPA with tumor growth.<sup>1,2</sup> On imaging, treatment naïve VSs can either demonstrate homogeneous or heterogeneous intratumoral enhancement and may contain hemorrhage or cystic changes. Edema of the adjacent parenchyma is seen in up to 40% of cases, particularly with large tumor size or rapid growth.<sup>3,4</sup> Symptoms of VSs most commonly encompass ipsilateral hearing loss and tinnitus. With increasing size, tumors may exert mass effect on adjacent

structures, resulting in trigeminal symptoms, hydrocephalus, and ataxia.<sup>5</sup>

A recent study described the presence of peritumoral hyperintense signal or “halo” around VSs on postcontrast 3D T2 FLAIR images. The authors of that study opined that this halo represented local leakage of gadolinium into the peritumoral space, though the mechanism remains unknown.<sup>9</sup> To date, however, investigation of this phenomenon has been limited and restricted to treatment-naïve patients. As such, the current study sought to further our knowledge of this subject by comparing the incidence and thickness of peritumoral halos in patients undergoing stereotactic radiosurgery (SRS).

## MATERIALS AND METHODS

### Eligibility Criteria

Local institutional review board approval was received before the study commencement. A retrospective review of patients with clinically presumed VSs was conducted based on imaging

Received May 15, 2024; accepted after revision January 9, 2025.

From the Departments of Radiology (S.T.N., J.C.B., G.B., P.J.F., J.I.L.), Otolaryngology-Head and Neck Surgery (M.L.C., M.J.L.), and Neurologic Surgery (M.L.C., M.J.L.), Mayo Clinic, Rochester, Minnesota.

Please address correspondence to John C. Benson, Department of Radiology, Mayo Clinic, 200 1st St SW, Rochester, MN 55905; e-mail: Benson.john3@mayo.edu  
<http://dx.doi.org/10.3174/ajnr.A8657>

## SUMMARY

**PREVIOUS LITERATURE:** This is a novel investigation of peritumoral hyperintense signal (a “halo”) around vestibular schwannomas in a patient cohort undergoing stereotactic radiosurgery.

**KEY FINDINGS:** Treated vestibular schwannomas tend to have great incidence of peritumoral “halo” with increased thickness compared with pretreatment lesions.

**KNOWLEDGE ADVANCEMENT:** Increased understanding of signal changes of vestibular schwannomas following SRS could relate to increased tumor permeability and may be a predictor of subsequent tumor shrinkage.

findings over 4 years (11/12/2019–8/23/2023). These tumors were treatment-naïve and subsequently underwent SRS. Treatment with SRS was planned with the 3D T1 postcontrast sequence coregistered to the contour of the 50% isodose line. Patients with dedicated IAC imaging before and following therapy were reviewed for appropriate pre- and postcontrast images for comparison. Patients were excluded for absence of necessary MR imaging sequences. Demographic information was acquired through the electronic medical record.

### MR Imaging Protocol

Patients were scanned with either a 3T Siemens or GE Healthcare scanner with multichannel phased array coils (and a 32- or 64-channel head coil). Twenty-three of the 26 patients underwent evaluation with a Siemens scanner both before and following SRS. One patient before SRS and 2 patients following SRS were imaged via a GE Healthcare scanner. Dedicated IAC imaging was performed utilizing axial 3D T1 sampling perfection with application-optimized contrasts by using different flip angle evolution (SPACE sequence; Siemens) (TR = 600 ms, TE = 32 ms, data matrix =  $192 \times 192$ , acquisition time = 4 minutes), axial 3D T2 SPACE (TR = 1300 ms, TE = 184 ms, data matrix =  $320 \times 320$ , acquisition time = 3 minutes 55 seconds), axial 3D fat-saturated postcontrast T1 SPACE (TR = 600 ms, TE = 32 ms, data matrix =  $192 \times 192$ , acquisition time = 4 minutes), and axial postcontrast 3D T2 FLAIR (TR = 5000 ms, TE = 379 ms, data matrix =  $192 \times 192$ , inversion time = 1700 ms, acquisition time = 4 minutes 29 seconds). The FOV was 150 for these sequences.<sup>10</sup> Images were acquired in the sequence noted above per institutional protocol and also included precontrast standard full brain sequences (ie, axial fat-saturated precontrast T2 FLAIR and sagittal precontrast T1 FLAIR). Gadobutrol (Gadavist) per weight-based table (0.1 mmol/kg) was administered via IV push for all the examinations. Axial 3D fat-saturated postcontrast T1 SPACE and, subsequently, axial postcontrast 3D T2 FLAIR were acquired following contrast injection. The order of the sequences was kept the same for all performed studies.

### Imaging Evaluation

Two experienced neuroradiologists (J.C.B., J.I.L.) performed the retrospective imaging review. The radiologists were blinded to the presence of recent treatment. VSs were evaluated for laterality—right or left—and location, described as in the IAC, CPA, or both. Before and following treatment, all VSs were measured in a single maximal axial dimension for size. If the VS involved

both the IAC and CPA, the largest single axial dimension of the CPA component was measured for standardization. Presence or absence of a fundal cleft was also reported, as well as a fundal cleft size between the lateral aspect of the VS and the IAC fundus.

VSs were evaluated for presence or absence of a peritumoral hyperintense signal on postcontrast 3D T2 FLAIR images (“halo”), before and after SRS, through the overlaying and fusion features of our PACS system (Visage, Version 7.1.18, Visage Imaging). Axial postcontrast 3D T2 FLAIR images were fused and overlaid with both axial fat-saturated postcontrast T1W1 and axial T2 SPACE images (Fig 1). Precontrast T2 FLAIR and postcontrast 3D T2 FLAIR were not directly comparable, and therefore, the halos could not be measured on precontrast images. Size or thickness of halo, if present, was measured through the differences in tumor size between the different sequences. The halos were measured perpendicular to the tumors. Though the halos were irregular in areas, the largest halo measurement for each tumor was recorded. Image subtraction was also utilized to better detect differences between the tumor margins and the peritumoral halo. Whether the peritumoral hyperintense signal was confined to the fundus was recorded. Halo thickness was averaged between the 2 observer measurements. Any disagreements between the observers for categorical variables were resolved by consensus.

### Statistical Analysis

For all continuous variables, means and SDs were calculated. Pearson  $\chi^2$  test was used to calculate statistically significant associations between the continuous variables. The Student *t* test was used to calculate statistical differences of the continuous variables. Cohen  $\kappa$  was used to calculate interrater reliability with categorical variables. *P* values < .05 were statistically significant.

## RESULTS

Twenty-six patients were included in the study, of which 14 were women (54.0%) and 12 were men (46.0%). Average age was 62 years (SD 12). Fourteen tumors were right-sided (56.0%), and 12 were on the left (46.0%). Of these, 8 (31%) tumors were restricted to the IAC, 1 (4%) was entirely situated in the cerebello-pontine angle, and 17 (65%) involved both regions. The tumors were Koos 1–4: 7 Koos 1 (27%), 11 Koos 2 (42%), 5 Koos 3 (19%), and 3 Koos 4 (12%). Average follow up period was 1.2 (SD 0.35) years or, on average, 14 months for each patient following initial baseline imaging. Pretreatment MRI studies were performed

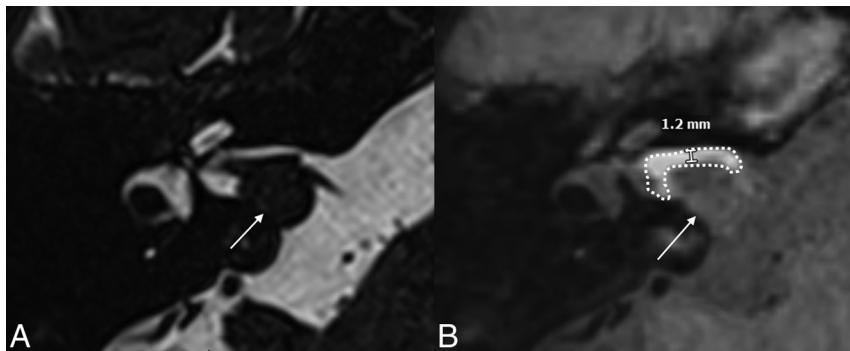


**FIG 1.** Evaluation and measurement of peritumoral halo. Axial T2 SPACE (A) and coregistered T2 SPACE and postcontrast 3D T2 FLAIR (B) images demonstrate a right-sided vestibular schwannoma (arrows) with peritumoral enhancement that is predominantly along the anterior margin of the tumor (dashed line). Measurement of the halo was performed perpendicular to the tumoral margin.

immediately before treatment. Postprocedural imaging was acquired approximately 10 (SD 2.4) months following end of treatment. Pretreatment VSs measured  $1.1 \pm 0.4$  cm, and post-treatment VSs measured  $1.3 \pm 3.3$  cm. Average tumoral size did not significantly change following treatment ( $P = .10$ ). Interobserver agreement on the presence of a halo before treatment was substantial ( $\kappa = 0.63$ ), whereas following treatment, it was moderate ( $\kappa = 0.56$ ).

Peritumoral halo on postcontrast 3D T2 FLAIR images ("halo") was seen in 85% of patients before treatment and 96% following SRS, with significant difference noted between pre- and posttreatment groups ( $P = .017$ ). Before treatment, peritumoral halos measured  $0.8 \pm 0.4$  mm in maximum thickness on average, which significantly increased in size following treatment ( $1.4 \pm 0.4$  mm) ( $P < .001$ ). Four of the VSs did not demonstrate a peritumoral halo before SRS (15.0%). Of these 4, 3 developed halos following treatment.

A fundal cleft was observed in 21 (81%) patients, with an average cleft size of  $1.7 \pm 1.1$  mm. The cleft size did not significantly change following treatment ( $P = .14$ ). Peritumoral halo was restricted to the fundus in 18 (69.0%) patients before SRS. None of the posttreatment patients had a halo restricted to the fundus. There was no correlation between the change in halo thickness and Koos classification.

## DISCUSSION

This study evaluated the changes in the incidence and thickness of peritumoral halos around VSs following SRS in a treatment-naïve cohort. The results indicate that peritumoral halos are more commonly seen around posttreatment tumors and are increased in thickness. The halos, when present, are also less likely to be restricted to the IAC fundus. Together, these findings indicate that the incidence, thickness, and locality of peritumoral halos around VSs change after SRS.

Stereotactic radiosurgery treatment combines delayed vascular and cytotoxic effects as described by Yang et al.<sup>11</sup> These delayed vascular effects pertain to radiation-induced damage to tumor nutrient vessels, critical for tumoral necrosis. The underlying abnormal vasculature of VSs is more susceptible to radiation-

induced sequelae than normal vessels. Cytotoxic effects relate to DNA damage from  $\gamma$  rays, generating oxygen free radicals and resultant strand breakage. The effects of SRS were studied on healthy rat brains, generating substantial vascular permeability about the area of treatment and the formation of new, leaky blood vessels seen on Gd-DTPA dynamic contrast-enhanced MRI and T2\*-weighted sequences.<sup>12</sup>

The most immediate implication of this study is that it offers further clues regarding the composition of peritumoral halos. Like the authors of the Benson et al<sup>9</sup> study, we hypothesize that the peritumoral halos could repre-

sent local extra-tumoral leakage of gadolinium. The observed changes in these halos following SRS might represent a greater degree of gadolinium leakage after SRS. Though the findings might reflect increased tumoral permeability, it is important to mention that no additional references have theorized increased vascular permeability as the etiology of the halo sign, and the appearance could also partly be due to accompanying inflammation. If that is the case, steroid use after treatment might have affected our results.

Steroids are not routinely prescribed in the early period after treatment. Though if a patient experiences a sudden sensorineural hearing loss in the post-SRS period (confirmed on audiogram), a course of steroids can be considered. In the uncommon case of a patient experiencing symptomatic brainstem edema after radiosurgery, steroids are used. In our cohort, no known steroid administration is documented to mitigate an inflammatory treatment response.

As first described, the peritumoral halos are often nonuniform in appearance and irregularly marginated. The authors of the original study on this concept hypothesized this irregularity could be explained by the trapping of gadolinium in the variably adhered and irregular arachnoid about the tumor.<sup>9</sup> It is possible that SRS leads to increased permeability and a larger concentration gradient of extravasated contrast, resulting in larger signal thickness. Extension of the peritumoral halo beyond the IAC might also be related to the internal necrosis of the tumor making it more "leaky." Post-SRS tumor necrosis is an important correlate of treatment effect and might have a correlation with the degree of increased peritumoral halo. Evaluation of this relationship was not within the scope of this study but is worthy of future analysis.

Next, as stated in the results, peritumoral halos were often restricted to the IAC in pretreatment tumors but were observed circumferentially around the tumors in posttreatment patients. Most likely, this is because local gadolinium leakage is easier to observe in the IAC in the presence of a VS, where it is entrapped, or at least partially entrapped, by mass effect related to the VS. In posttreatment tumors, conversely, the increased permeability allows for observation of a halo even in regions that are not



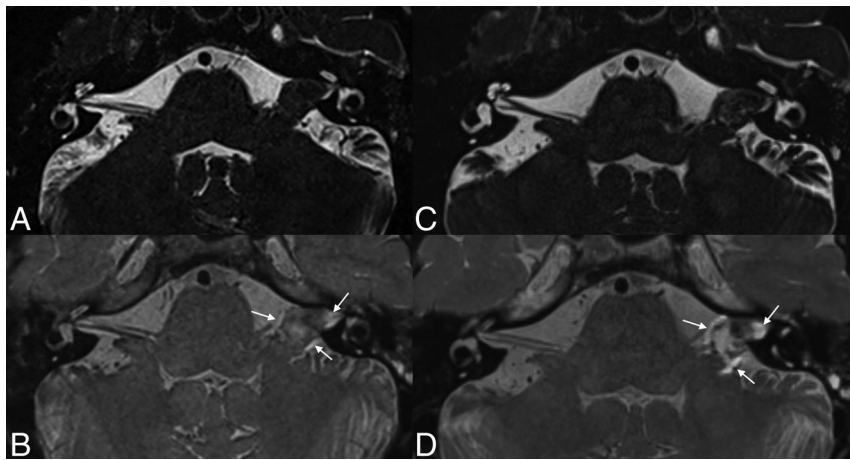


**FIG 2.** Increased size of a peritumoral halo in a 68-year-old woman. Preradiosurgery axial T2 SPACE (A) and postcontrast 3D T2 FLAIR (B) images demonstrate a small halo located circumferentially around a left VS (arrows on B). Postradiosurgery axial T2 SPACE (C) and postcontrast 3D T2 FLAIR (arrows, D) images show that the halo has increased in size following treatment.

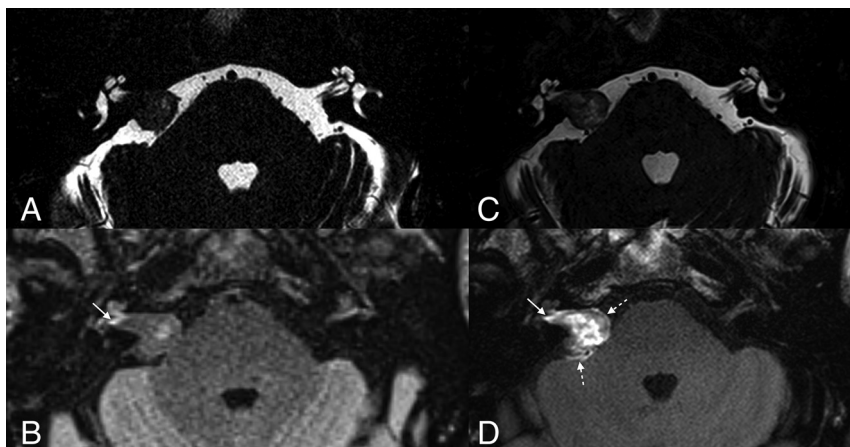


**FIG 3.** Increased halo size following SRS in a 66-year-old man. Pre-SRS axial T2 SPACE (A) and postcontrast 3D T2 FLAIR (B) images demonstrate minimal halo that is restricted to the IAC fundus (solid arrow, B). Following treatment, axial T2 SPACE (C) and postcontrast 3D T2 FLAIR (D) images show that the involvement of the fundus has increased (solid arrow, D). There is also a new circumferential halo elsewhere (dashed arrows, D).

entrapped, such as the cerebellopontine angle and cerebellum (Figs 2 and 3).

It is interesting to speculate that, if indeed, the halo corresponds to gadolinium leakage, its increase following treatment could reflect increased tumor permeability and may be a predictor of subsequent tumor shrinkage following SRS. Though we found no significant change in size of tumor after SRS in our small cohort, our follow-up period was less than 2 years. A longer follow-up period (potentially at least 3 years, as seen in a study performed by Lipski et al<sup>13</sup>) may be needed to see treatment response as it relates to tumor control and shrinkage, despite increased halo thickness and possible associated tumor permeability presenting within 2 years following treatment. Further study with a larger number of tumors over a longer imaging interval will be needed to determine if this might prove to be the case.

This study has several limitations given its retrospective nature. The results are based on a small cohort, and a larger sample size is needed to validate these findings and the overall clinical significance. Longer follow-up periods than what is seen in our cohort may also be helpful to evaluate for presence or absence of communicating hydrocephalus, change in tumor size, and temporal evolution of halo thickness and morphology, as well as clinical impact relating to sensorineural hearing loss, tinnitus, and vertigo. Unlike in our prior investigations, patients were selected for the availability of appropriate pre- and post-contrast imaging before and after treatment, which resulted in several patient exclusions for missing imaging. There are also inherent technical differences across multiple manufacturers, such as GE Healthcare and Siemens, which can be more challenging in direct comparison. Finally, the small average halo thickness of reported measurements—between 0.4 and 1.5 mm before treatment and 0.4 and 2.6 mm after SRS—may be challenging because of pixel size on standard PACS measuring tools. It is worth noting that the voxel dimension is 0.78 mm ( $192 \times 192$  acquisition matrix with FOV 150), and the average increase in halo thickness from pre- to posttreatment was 0.6 mm and, therefore, smaller than the acquired voxel.

## CONCLUSIONS

VSs treated with stereotactic radiosurgery are more likely to have a peritumoral halo on postcontrast 3D T2 FLAIR images, with larger halo sizes as

compared with pretreatment studies. Further study with a larger tumor cohort and longer follow-up will be necessary to determine if these findings are predictive of subsequent tumor shrinkage.

Disclosure forms provided by the authors are available with the full text and PDF of this article at [www.ajnr.org](http://www.ajnr.org).

## REFERENCES

1. Lin EP, Crane BT. **The management and imaging of vestibular schwannomas.** *AJNR Am J Neuroradiol* 2017;38:2034–43 [CrossRef Medline](#)
2. Connor SE. **Imaging of the vestibular schwannoma: diagnosis, monitoring, and treatment planning.** *Neuroimaging Clin N Am* 2021; 31:451–71 [CrossRef Medline](#)
3. Bonneville F, Savatovsky J, Chiras J. **Imaging of cerebellopontine angle lesions: an update, Part 1: enhancing extra-axial lesions.** *Eur Radiology* 2007;17:2472–82 [CrossRef Medline](#)

4. Thamburaj K, Radhakrishnan VV, Thomas B, et al. **Intratumoral microhemorrhages on T2\*-weighted gradient-echo imaging helps differentiate vestibular schwannoma from meningioma.** *AJNR Am J Neuroradiol* 2008;29:552–57 [CrossRef Medline](#)
5. Gurewitz J, Schnurman Z, Nakamura A, et al. **Hearing loss and volumetric growth rate in untreated vestibular schwannoma.** *J Neurosurg* 2022;136:768–75 [CrossRef Medline](#)
6. Tanaka Y, Kobayashi S, Hongo K, et al. **Clinical and neuroimaging characteristics of hydrocephalus associated with vestibular schwannoma.** *J Neurosurg* 2003;98:1188–93 [CrossRef Medline](#)
7. Fukuda M, Oishi M, Kawaguchi T, et al. **Etiopathological factors related to hydrocephalus associated with vestibular schwannoma.** *Neurosurgery* 2007;61:1186–92 [CrossRef Medline](#)
8. Al Hinai Q, Zeitouni A, Sirhan D, et al. **Communicating hydrocephalus and vestibular schwannomas: etiology, treatment, and long-term follow-up.** *J Neurol Surg B Skull Base* 2013;74:68–74 [CrossRef Medline](#)
9. Benson JC, Carlson ML, Lane JI. **Peritumoral signal on postcontrast FLAIR images: description and proposed biomechanism in vestibular schwannomas.** *AJNR Am J Neuroradiol* 2023;44:1171–75 [CrossRef Medline](#)
10. Benson JC, Carlson ML, Lane JI. **MRI of the internal auditory canal, labyrinth, and middle ear: how we do it.** *Radiology* 2020;297:252–65 [CrossRef Medline](#)
11. Yang SY, Kim DG, Chung HT, et al. **Evaluation of tumour response after gamma knife radiosurgery for residual vestibular schwannomas based on MRI morphological features.** *J Neurol Neurosurg Psychiatry* 2008;79:431–36 [CrossRef Medline](#)
12. Constanzo J, Masson-Côté L, Tremblay L, et al. **Understanding the continuum of radionecrosis and vascular disorders in the brain following gamma knife irradiation: an MRI study.** *Magn Reson Med* 2017;78:1420–31 [CrossRef Medline](#)
13. Lipski SM, Hayashi M, Chernov M, et al. **Modern gamma knife radiosurgery of vestibular schwannomas: treatment concept, volumetric tumor response, and functional results.** *Neurosurg Rev* 2015; 38:309–18; discussion 318 [CrossRef Medline](#)